CHEMISTRY OF MATERIALS

Article

pubs.acs.org/cm

Graphene-like Molecules Based on Tetraphenylethene Oligomers: Synthesis, Characterization, and Applications

Ji Ma,[†] Tingting Lin,[‡] Xiaoyong Pan,[‡] and Weizhi Wang*,[†]

[†]State Key Laboratory of Molecular Engineering of Polymers, Department of Macromolecular Science, Fudan University, Shanghai 200433, P. R. China

[‡]Institute of Materials Research and Engineering, A*STAR (Agency for Science, Technology and Research), 3 Research Link, Singapore 117602, Singapore

Supporting Information

ABSTRACT: Graphene-like molecules were prepared by oxidative cyclodehydrogenation of tetraphenylethene(TPE) oligomers using iron(III) chloride as the catalyst under mild conditions. All the oxidized samples can be separated effectively from the stepwise ring-closing reaction that highly related to the reaction time. For example, the model compounds obtained from the stepwise cyclization reaction show a regular red-shift in UV/vis absorption and photoluminescence (PL) spectra. This result reveals that the molecular conjugation length will extend with the stepwise ring-closing reaction going on. Interestingly, we successfully obtained a series of colorful luminogens with blue, cyan, and green emission during this stepwise and accurate ring closing process. Cyclic voltammetry measurements taken give the corresponding band gap, which supports the results obtained from optical spectroscopy. For the strong intermolecular interaction, our graphene molecules can self-assemble to form a red-colored and hexagonal fiber. Furthermore, some molecules exhibit piezochromic luminescence. The PL emission of the molecules before and after oxidation can be dramatically quenched by picric acid through the electron transfer and/or energy transfer mechanism, enabling them to function as chemosensors for explosive detection. In addition, fluorescence cell imaging studies proved their potential biological application.

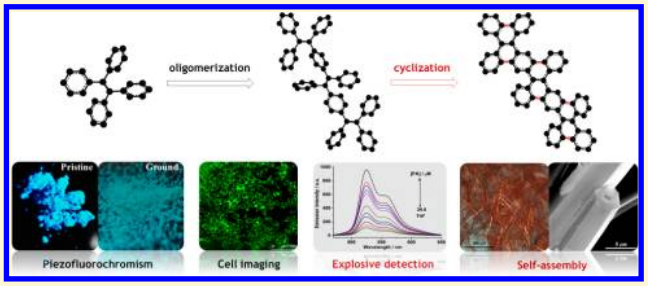

INTRODUCTION

Graphene,[1,2] a two-dimensional (2D) material, has drawn worldwide attention and demonstrated extraordinary promise in nanoelectronics, optical limiters, biosensors, supercapacitors, and polymer nanocomposites due to its exceptional electronic,[3,4] thermal,[5] optical,[6−9] and mechanical properties.[10] Inspired by these fascinating properties and enormous potential applications, many efforts have been devoted to the preparation of graphene in recent years.[11−15] Approaches for synthesizing graphene can be generally divided into two major groups: top-down and bottom-up. Top-down techniques consist, for example, of micromechanical exfoliation,[16] organic solvent-assisted exfoliation,[17] electrochemical exfoliation,[18] etc. Bottom-up methods mainly involve chemical vapor deposition,[19,20] epitaxial growth on silicon carbide,[21,22] and self-assembly of surfactants,[23] which can start from carbon precursors of small and well-defined size. Beyond the above-mentioned approaches, the total organic synthesis of polycyclic aromatic hydrocarbons (PAHs) can be regarded as a new method to prepare graphene.[24,25] Early in the first half of the 20th century, Scholl, Clar, and Zander et al. have made pioneering contributions to the synthesis and structural characterization of various PAHs.[26−29] In order to overcome the complicated experimental workup and the low yield of the desired compound, Müllen and co-workers have developed an efficient way to prepare well-defined PAHs by oxidative cyclodehydrogenation. In this example, oligophenylene is used as the potential graphene−molecule precursor catalyzed by the iron(III) chloride ($FeCl_3$)/nitromethane (CH_3NO_2) system.[30,31] In 2011, Rathore and co-workers[32] gave us another example that tetraphenylethylenes (TPEs) can be oxidatively transformed into dibenzochrysenes by the 1,2-dichloro 4,5-dicyanoquinone (DDQ)/H^+ system. Inspired by the above two examples: Is it possible to obtain the graphene molecules from TPEs through the cyclization reaction?

TPEs, which have exceptional electronic behaviors[33,34] and excited state properties,[35−37] have drawn much attention due to their potential application in optoelectronic and optomechanical switching, storage devices, and sensitive fluorescent chemosensors.[38−40] Since the unusual phenomenon of aggregation-induced emission (AIE) was first reported by Tang's group in 2001, studies on TPE have become more and more intense owing to its great simplicity in synthesis and derivatization.[41,42] Meanwhile, various TPE derivatives, consisting of multiple phenyl rotors and olefinic stators, are prepared, which are highly emissive in their aggregated form

Received: May 2, 2014
Revised: June 26, 2014
Published: June 30, 2014

ACS Publications © 2014 American Chemical Society

dx.doi.org/10.1021/cm501590w | Chem. Mater. 2014, 26, 4221−4229

Scheme 1. Synthetic Routes for Compounds 4c−6c

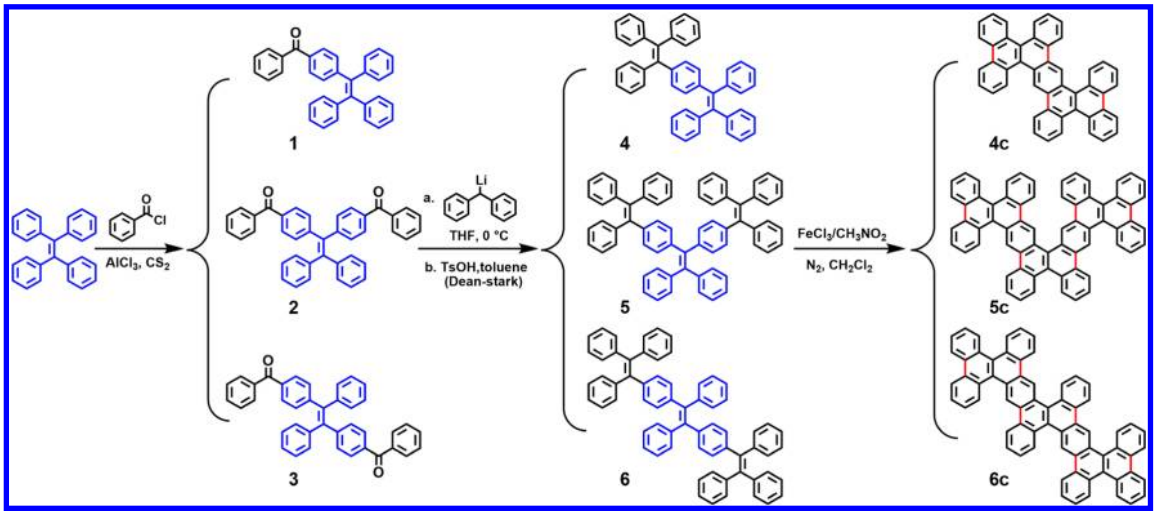

compared with their weak emission in solution because the fast internal rotation of the phenyl rings and partial twisting of the C=C bond deactivate the excited state via the nonradiative decay channels.[43−47] On the basis of the current understanding, restriction of intramolecular rotation has been proposed to be the main cause for the AIE effect.[48] To date, in order to verify this hypothesis, great efforts have been devoted to it by researchers.[49−54] As one important example, the TPE-based molecule with an oxygen bridged ring-closed structure was designed and synthesized, which provides a direct explanation for the structure−property relationships.[55] Herein, we straightforwardly locked the phenyl rings of the twisted TPE-based oligomers with a covalent linkage (carbon−carbon single bond) and readily obtained near-planar aromatic hydrocarbons using $FeCl_3$ as the catalyst. Accordingly, the light emissions, electronic properties, and intermolecular interactions can be well-tuned by modifying the chemical structure of the extended π-conjugated molecules. From another perspective, such $FeCl_3$-catalyzed oxidations of TPE-based oligomers to graphene molecules were rarely reported. This may afford a total organic synthetic approach to obtain the well-defined and nanosized graphene-like materials by appropriate TPEs precursors.[56,57] Namely, this may achieve atomically precise bottom-up fabrication of nanoribbons with different topologies and widths.[58] Interestingly, we successfully obtained two partially ring-closed intermediates with different emission colors, which indicated that the cyclization reaction is a stepwise and controllable process. On the basis of this result, a detailed relationship between the number of restricted phenyl rings and optical properties of luminogens can be found. Meanwhile, we can further decipher how the conjugation or conformation of the molecules affects their photo properties and explore their potential applications in the fields of fluorescent chemosensors and stimuli-responsive materials. In addition, the fluorescent images and cytotoxicity assay of the as-synthesized molecules are presented to demonstrate their potential as targeted probes for optical bioimaging.

EXPERIMENTAL SECTION

Materials. Chemicals and reagents were purchased from Aldrich or Acros Chemical Co. unless specifically stated. THF was distilled under nitrogen from sodium benzophenone ketyl immediately prior to use. All other solvents were of analytical grade and were purified using standard methods.

Instruments. ^1H and ^{13}C NMR spectra were measured on Varian Mercury Plus 400 spectrometer in deuterated dichloromethane (CD_2Cl_2), and chemical shifts were reported in ppm units with tetramethylsilane (TMS; δ = 0 ppm) as an internal standard. High-performance liquid chromatography (HPLC) was performed on a Shimadzu system (LC-10 ADVP, Kyoto, Japan). UV/vis absorption spectra (UV) spectra were obtained in distilled dichloromethane on a Shimadzu UV-3150 spectrophotometer. Fluorescence spectra (PL) were measured on a Shimadzu RF-5310 PC fluorometer at room temperature. The PL quantum yields (Φ_F) were estimated using quinine sulfate (Φ_F = 54% in 0.1 M H_2SO_4) or fluorescein (Φ_F = 92% in 0.1 M NaOH) as standards. PL lifetimes were recorded on FLS920 spectrofluorometer (Edinburgh Instruments, U.K.) using a time-corrected single photon counting system at room temperature. The samples were analyzed by Voyager DE-STR matrix assisted laser desorption time-of-flight mass spectrometry (MALDI-TOF). Elemental analysis was performed on a VARIO EL3 instrument (ELEMENTAR, Germany). Polarizing microscope images were obtained using DM2500P. Scanning electron microscope (SEM) images were examined by TESCAN VEGA TS 5136MM. Cyclic voltammetry (CV) was carried out on a T30/FRA2 electrochemical workstation. CV measurements of the oligomer films coated on a glassy carbon electrode (0.08 cm^2) were performed in an electrolyte of 0.1 M tetrabutylammonium hexafluorophosphate ($TBAPF_6$) in acetonitrile using ferrocene (FOC) (4.8 eV under vacuum) as the internal standard at a scan rate of 100 mV s^{-1} at room temperature under the protection of argon. The counter electrode was a platinum wire, and an $Ag/AgNO_3$ electrode was used as the reference electrode. Differential scanning calorimetry (DSC) was carried out using a Q2000 DSC instrument at a scan rate of 10 °C min^{-1}. Powder X-ray diffraction (XRD) patterns were conducted on an X'Pert-Pro MPD diffractometer with Cu Kα radiation (λ = 1.5418 Å) at 25 °C (scan range: 5−45°). X-ray crystallographic data were collected on a P4 Bruker diffractometer equipped with a Bruker SMART 1K CCD area detector (employing the program SMART) and a rotating anode utilizing graphite-monochromated Mo Kα radiation (λ = 0.71073 Å). Data processing was carried out by use of the program SAINT, while the program SADABS was utilized for the scaling of diffraction data, the application of a decay correction, and an empirical absorption correction based on redundant reflections. The structures were solved by using the direct-methods procedure in the Bruker SHELXL program library and refined by full-matrix least-squares methods on F2. All non-hydrogen atoms were refined using anisotropic thermal parameters, and hydrogen atoms were added as fixed contributors at calculated positions, with isotropic thermal parameters based on the carbon atom to which they are bonded.

dx.doi.org/10.1021/cm501590w | Chem. Mater. 2014, 26, 4221−4229

Cell Culture and Imaging. The L929 cells were cultured in minimum essential medium containing 10% fetal bovine serum and antibiotics (100 units mL^{-1} penicillin, 100 μg mL^{-1} streptomycin) in a 5% CO_2 humidity incubator at 37 °C. The L929 cells were grown overnight on a plasma-treated 25 mm round coverslip mounted onto a 35 mm Petri dish with an observation window. The living cells were stained with the luminogens **4** or **4b** at concentrations of 20 μM (by adding 8 μL of a 5 mM stock solution of samples in DMSO to 2 mL of culture medium) and maintained at 37 °C in an atmosphere of 5% CO_2 and 95% air for an incubation time of 4 h. The cells were then washed with PBS twice, and 3 mL of PBS was added to each well. The cells were imaged using a confocal laser scanning microscopy (Olympus FV1000 laser scanning microscope) and a 60-oil-immersion objective lens. Cells stained with luminescent materials were excited at 488 and 543 nm.

Cell Viability by MTT Assay. The MTT assay was performed to ascertain the cytotoxic effect of the compounds' treatment. Prior to being tested, 1×10^4 cells were seeded per well in a 96-well plate. After overnight culture, different concentrations of **4** or **4b** were added into the 96-well plate for 24 h. After treatment, the medium was aspirated and 100 μL of fresh medium with 10% FCS was added to each well with a MTT stock solution (10 μL, 5 mg mL^{-1}). Cells were cultured for 4 h at 37 °C. Afterward, the medium was removed, and the cells were lysed with DMSO (100 μL per well). A Molecular Devices SpectraMax M5Microplate Reader was used to measure the absorbance at 490 nm. Each of the experiments was performed at least three times.

RESULTS AND DISCUSSION

Synthesis. To understand the structure−property relationship, we used an efficient reaction route for preparing a variety of near-planar molecules via a mild intramolecular oxidative cyclodehydrogenation. Herein, the $FeCl_3/CH_3NO_2$ system was utilized for these transformations, which has been used in the synthesis of PAHs because of refraining from severe disadvantages such as dealkylation, chlorination, or even migration of the alkyl substituents.[31] In this study, we carefully controlled the quantity of oxidant and the time of reaction. The molecules with less twisted conformation were synthesized in quantitative yield (Scheme 1). Intriguingly, the partially ring-closed intermediates **4a**, **4b**, and **4c** have been separated and successfully characterized, as shown in Scheme 2. This result

Scheme 2. Oxidation of Compound 4 in a Stepwise Process

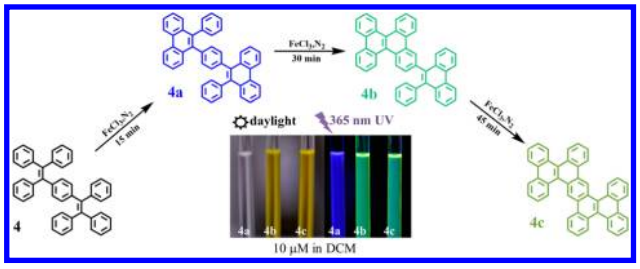

can further support a stepwise ring-closing mechanism proceeding from **4**−**4c**, and this simple synthetic procedure enabled us to manipulate its molecular structure and alter its emission property easily. Similarly, it is presumable that the oxidation of **5** and **6** also underwent the same transformation way.

All intermediates and final products were carefully purified and further characterized by NMR, mass spectrometry, and elemental analysis (see Supporting Information for detail). Single crystals of compounds **1** and **6** were isolated from their dichloromethane (DCM)/methanol solutions and were characterized by X-ray crystallographic analysis (Figure 1 and Table S1 in the Supporting Information). The molecule **5** showed

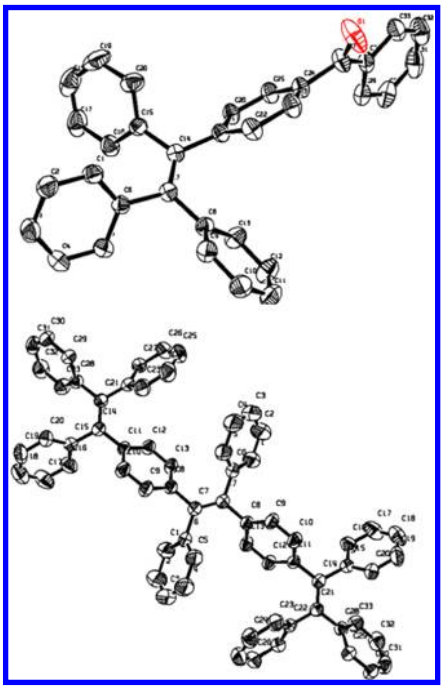

Figure 1. ORTEP drawings of compounds **1** and **6** at the 30% probability level; hydrogen atoms are omitted for clarity.

different dissolvability relative to its isomer **6**. We explained that the twisted conformation of compound **6**, which can reduce intermolecular interactions and generate large free volume to accommodate more solvent molecules, affords its better solubility than compound **5**.

Self-Assembly. Small molecules with the macroscopic self-assembly behavior always show a lot of unique and enhanced properties.[59−61] Recently, researchers suggest that the strong $\pi-\pi$ stacking between planar, organic small molecules can be as effective as driving the aromatic molecules to assemble into one-dimensional macrostructure relative to other weak interactions or hydrogen bonding.[62] As noted above, a group of small molecules with twisted structure were readily oxidized to several less twisted products by the C—C bond forming reaction. To our surprise, the near-planar and linear molecule **6c** tended to evidently aggregate at the solvent interface, which can be seen with the naked eye, when a poor solvent, such as methanol, was dropped slowly into its DCM solution in a beaker (Figure 2a). When the flocculent aggregation was picked up carefully with a metal needle, as shown in Figure 2b, it can be pulled to form a red fiber with lengths of several millimeters due to the strong intermolecular cofacial π-stacking between adjacent molecules. After the slow solvent evaporation at ambient temperature, precipitates were obtained at the bottom of the beaker; the polarizing microscope image is shown in Figure 2c, numerous regular microscale fibers were observed, and the typical diameters were several micrometers. In other words, the sample **6c** with the extended π-systems in only one direction showed a good self-assembling ability in a mixed solvent of DCM/methanol through the strong $\pi-\pi$ stacking among the almost planar π-layers. To further identify its microstructure, scanning electron microscope (SEM) investigation was carried out. Intriguingly, the shape of the

dx.doi.org/10.1021/cm501590w | Chem. Mater. 2014, 26, 4221−4229

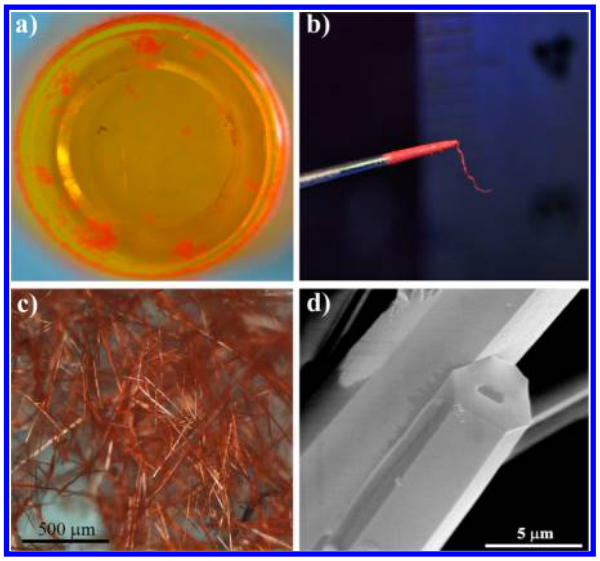

Figure 2. Images of (a) the aggregate formation of compound **6c** and (b) the fiber pulled from the DCM/methanol mixture; (c) polarizing microscope image and (d) SEM micrograph of fibers of **6c** obtained from DCM solution.

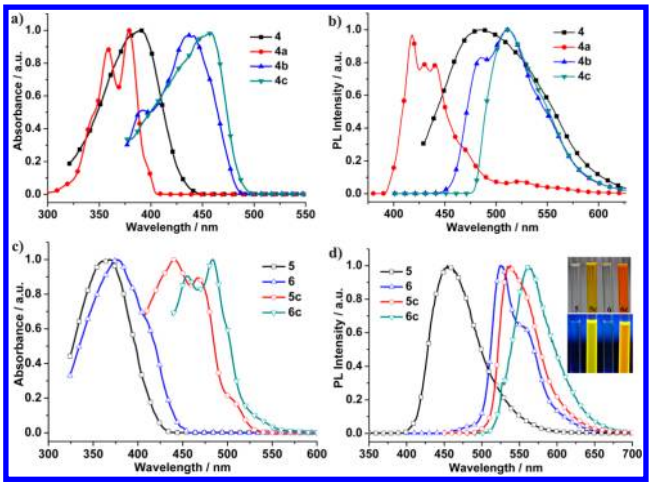

Figure 3. (a) Normalized absorption and (b) PL spectra of **4**–**4c** in DCM solutions (10 μM). (c) Normalized absorption and (d) PL spectra of **5**–**6c** in DCM solutions (10 μM). Inset in panel d: photos of luminogens **5**–**6c** under room light (up) and 365 nm UV light (down).

microfibers was irregular hexagon-like which was different from other ordered one-dimensional microstructures such as ribbons, wires, and rods that had been reported (Figure 2d). However, we don't observe the similar interesting result when molecules **4c** and **5c** were used in the assembly process. So the assembly behavior of the graphene-like molecules must be related to the length–diameter ratio of the molecule. To our knowledge, self-assembly is an alluringly inexpensive route to pattern the integrated nano- or micro-optoelectronics. For this reason, one-dimensional organic microfiber self-assembled from compound **6c** can be a promising building block in organic field-effect transistors. The corresponding experiment is currently in progress in our laboratory.

Optical Properties. To investigate the changes in optical properties after locking the phenyl rings of compound **4** in a stepwise process and learn how subtle structural change modulates the emission color, UV/vis absorbance and PL emission spectra of **4**–**4c** in their dilute DCM solutions were obtained (Figure 3). Absorption peaks of **4**–**4c** were respectively located at 390, 379, 437, and 457 nm, associated with large molar extinction coefficients, which were collected in Table S2 in the Supporting Information. Compound **4** in dilute DCM solution emits almost no light under UV irradiation because the motions of the multiple phenyl blades against the ethylene core nonradiatively deactivated its excited states. However, the oxidized luminogens can strongly emit in DCM solution. The corresponding values of PL curves of **4a**–**4c** have maxima at 437, 509, and 513 nm, respectively, which were located in the blue to green spectral region, and the Stocks shifts for **4a**–**4c** were 62, 72, and 56 nm, respectively, indicating of conformational reorganization in geometry from the pyramidal ground state to a more planar exicited state.[47] Intriguingly, the DCM solution of **4a** can emit deep blue light under the UV lamp after only two new C–C bonds were formed. This may be attributed to the blocking of the nonradiative pathway through locking of the rotation of the phenyl rings. By further locking of the phenyl rotors by the covalent linkage, we finally obtained **4b** and **4c** luminogens. Meanwhile, we can observe an obvious difference that the maximum emissions in the PL spectra have a clear red-shift with the increase of the locked phenyl ring number. The reason is that extending the effective conjugation length can increase the extent of π-electrons delocalization and narrow the molecular electronic energy level, resulting in a red-shift in fluorescence emission. The final oxidized compound **4c**, which had a big red-shift (76 nm) compared to **4a**, can emit green fluorescence in solution under UV irradiation. In other words, we successfully used a simple method to obtain three different emission colors (blue, cyan, and green) by controlling the number of restricted phenyl rings in one system (Scheme 2). To provide further evidence for the above discussion, the quantum yields (Φ_F) and PL lifetime of **4**–**4c** were conducted. The Φ_F of **4** (2.98%) is small because the intramolecular rotation of the multiple phenyl rings nonradiatively deactivated its excited states. The Φ_F for compounds **4a**, **4b**, and **4c** were 8.47%, 53.29% and 64.29%, respectively, suggesting that the Φ_F can be gradually increased with the number of locked phenyl rings, which coincided well with their different emission colors and PL spectra in solutions. Also, it is clear that the PL lifetime (τ) increased from 1.28, 2.02, and 8.93 to 9.11 ns for **4**, **4a**, **4b**, and **4c**, respectively, indicating that the excited species of the luminogens in solution can relax much more slowly by restriction of intramolecular rotation step by step, nicely correlating with the change of Φ_F.

Similarly, we oxidized the twisted luminogen **5** to a nearly planar compound **5c** by $FeCl_3$ catalyst. Compound **6** was given the same treatment. Luminogens **5** and **6** are practically nonemission in the monomeric state when dissolve in good solvent. It has been elucidated that luminogens **5** and **6** in DCM solution exhibit unrestricted internal bond motions, resulting in poor fluorescence efficiencies. When the internal bond motions were restrained by locking the rotation of the phenyl rings, they emitted strongly in a dilute DCM solution (the inset in Figure 3d), and their UV curves are shown in Figure 3c. The PL spectra of **5c** and **6c** in DCM solution peaked at 539 and 563 nm, which are 84 and 39 nm largely red-shifted from those of **5** and **6**, indicative of a longer conjugation length in the nearly planar molecules. Whereas the Stocks shift for **6** was 151 nm, the other three molecules (**5**, **5c**, and **6c**) exhibited Stokes shifts of 83–97 nm, suggesting that there is a

dx.doi.org/10.1021/cm501590w | *Chem. Mater.* 2014, 26, 4221–4229

large and fast change in geometrical structures upon excitation. In addition, the Φ_F and PL decay times for the cyclized compounds are dramatically enhanced compared to the values of twisted TPE-based oligomers due to the restriction of the phenyl rings rotations and the reduced nonradiative deactivation process (Table S1, Supporting Information).

We continued to research the PL behaviors of **5**−**6c** in the solid state. The solid films were obtained by spin-coating a DCM solution with a concentration of 100 m. The film emissions of **5**, **5c**, and **6c** were located at 485, 565, and 605 nm, which were 28, 26, and 42 nm red-shifted from those of the solutions, respectively, whereas compound **6** exhibited a 23 nm blue shift compared to its PL peak in solution (Figure 4). In

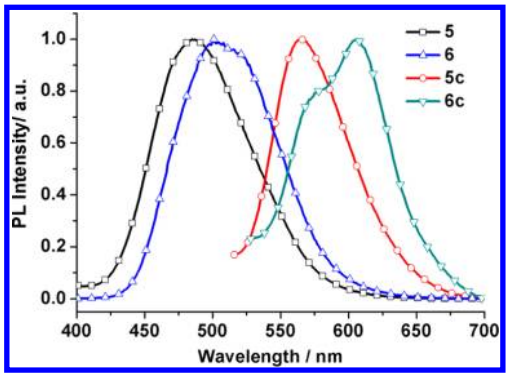

Figure 4. Normalized PL spectra of solid thin films of **5**−**6c**.

our general understanding, aggregation can induce the coplanarization of chromophores, which can lead to a better conjugation, thus redshifting its emission. Why this unusual emission occurred? It could be explained that compound **6** adopts a more twisted conformation in the solid state compared with that in its solution, as shown in the single-crystal X-ray structure of **6** (Figure 1). This would lead to a weaker intramolecular electron donor−acceptor interaction and a blue shift in its emission.

Electrochemical Properties. In order to better understand the relationship between the electronic structure and optical properties and to explain the pronounced fluorescence red shift, cyclic voltammetry (CV) measurements of the as-synthesized compounds were carried out. It is well-known that the highest occupied molecular orbital (HOMO), lowest unoccupied molecular orbital (LUMO), and energy band gaps (ΔE_g) are three important parameters for electroluminescent materials. As an example, the CV curves of compounds **6** and **6c** are shown in Figure S1 in the Supporting Information.

The electrochemical properties, as well as the energy level parameters of the synthesized compounds, are listed in Table 1. We can estimate the HOMO energy levels of compounds **4**−**4c** to be −5.62, −5.81, −5.46, and −5.44 eV, respectively, based on their onset oxidation potentials (1.06 to 0.69 V). The energy band gaps (ΔE_g) of **4**−**4c** are calculated to be 2.86, 3.06, 2.58, and 2.52 eV, which can be determined from the onset wavelength of their UV absorptions. The LUMO values ranged from −2.75 to −2.92 eV. Similarly, the corresponding values of the HOMO energy levels and band gaps of **5**−**6c** are shown in Table 1. The experimental band gaps match very well with the UV date and the molecular extended conjugation length.

Piezofluorochromism. Stimuli-responsive luminescent materials with a color-changeable property have drawn much attention because of their potential application in sensors,[63−65]

Table 1. Electrochemical Properties of Samples 4-6c[a]

compound	$E_{onset\text{-}ox}$ (V)	HOMO (eV)	λ_{onset} (nm)	ΔE_g (eV)	LUMO (eV)
4	0.87	−5.62	433	2.86	−2.76
4a	1.06	−5.81	405	3.06	−2.75
4b	0.71	−5.46	481	2.58	−2.88
4c	0.69	−5.44	492	2.52	−2.92
5	0.78	−5.53	423	2.93	−2.60
5c	0.61	−5.36	513	2.42	−2.94
6	0.75	−5.50	436	2.84	−2.66
6c	0.58	−5.33	522	2.37	−2.96

[a]Abbreviations: $E_{onset\text{-}ox}$ = onset oxidation potential determined from cyclic voltammetry in acetonitrile for oxidation potentials (0.1 M *n*-$Bu_4N^+PF_6^-$ as a supporting electrolyte) using Ag/Ag+ as a reference electrode at a scan rate of 100 mV s^{-1}. HOMO is derived by the equation HOMO = $-e(E_{onset\text{-}ox} - 0.0468\ V) - 4.8$ eV, where the value 0.0468 V is for FOC vs Ag/Ag^+. λ_{onset} = onset absorption wavelength, LUMO = ΔE_g + HOMO.

memory,[66] and security inks.[67] In general, these smart luminogens always exhibit morphology dependent fluorescence when treated with a mechanical stimulus such as grinding, shearing, or pressing—a phenomenon called piezochromic luminescence.[68,69] To our knowledge, altering the physical molecular packing pattern is easier to modulate the solid-state emission than changing the molecular chemical structures. Several types of luminogens have been reported to exhibit piezofluorchromic properties.[70−73] Some luminogens can switch their emissions by changing their aggregates between amorphous and crystalline in response to external pressure by grinding.[74−77] Herein, we investigated whether these as-synthesized samples of **1**−**6** have the piezofluorochromic properties. After a careful examination, three of the compounds (**1**, **4**, and **5**) exhibited obvious piezofluorochromic behavior.

The as-synthesized sample of **1** was an opaque crystal, and when irradiated with a 365 nm UV lamp, it emitted a strong blue light (Figure 5a). When compound **1** was ground using a mortar and a pestle for a moment, it became a light green powder and showed dark cyan emission under the UV lamp, as shown in Figure 5c. The PL spectrum of the ground sample exhibited a large red shift of 50 nm from 461 to 511 nm (Figure

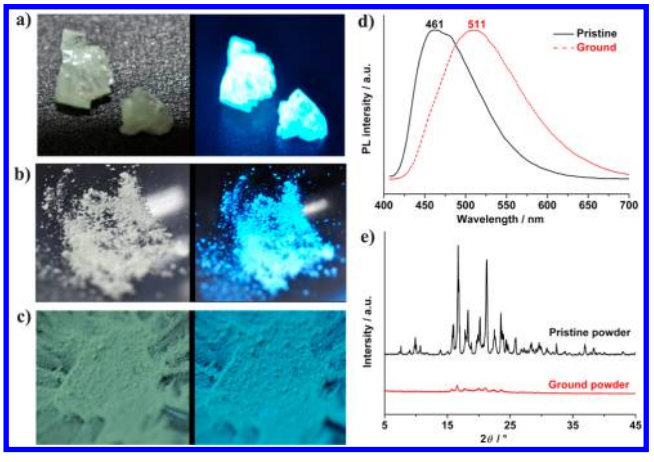

Figure 5. Photos of compound **1** of (a) the pristine crystal, (b) the pristine powder, and (c) the ground powder under room light (left) and 365 nm UV light (right). (d) PL spectra (excitation wavelength: 397 nm) and (e) powder X-ray diffraction patterns of the pristine powder and the ground powder.

dx.doi.org/10.1021/cm501590w | *Chem. Mater.* 2014, 26, 4221−4229

5d), revealing that this compound has piezofluorochromic behavior. To further unveil the mechanism of the mechanochromic fluorescence, powder X-ray diffraction (XRD) and differential scanning calorimetry (DSC) measurements were carried out on the pristine crystal and the ground powder of compound **1**. According to the powder XRD patterns (Figure 5e), compound **1** showed different structures of molecular assemblies before and after grinding. The diffraction curve of the original crystal displays many sharp and intense reflections, which are indicative of some crystalline orders. The diffraction curve of the ground powder shows weak reflections that agree with those of the original crystal, indicative of a not absolutely amorphous phase due to the spontaneous recovery during grinding. The DSC curve of the ground powder from compound **1** shows a broad exothermic peak at around 76 °C before melting, which is absent in the DSC thermogram of pristine crystal (Figure 6), revealing that the ground sample is

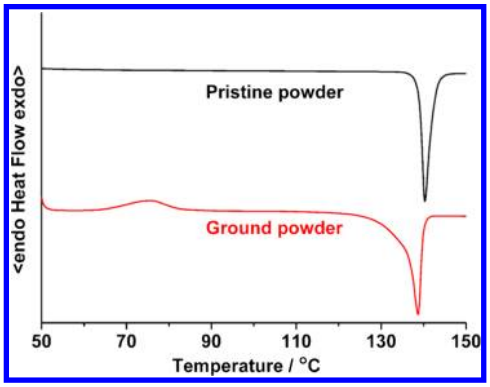

Figure 6. DSC thermograms of pristine powder and ground solid of compound **1**.

in a metastable amorphous state and can crystallize promptly in the solid state upon heating. Thus, it is clear that the molecular packing patterns of luminogen **1** can transform from the crystalline to the amorphous phase by grinding.

Similar to compound **1**, luminogens **4** and **5** can also emit two different lights at different conformation of molecular assemblies. Upon exciting with UV light, both compound **4** and compound **5** exhibit strong blue emissions as shown in Figure S2 and Figure S3 in the Supporting Information, with peaks locating at 458 and 460 nm in their PL spectra, respectively. After the grinding treatment, the produced compounds **4** and **5** emit green and yellow-green light under UV irradiation, and peaks centered at 498 and 504 nm, respectively. The red shift of the emission peaks of compound **4** and compound **5** before and after grinding are 40 and 44 nm, respectively. It is well-known that the grinding may destroy the crystals, whose conformations are more twisted than those in the amorphous phase, thus triggering planarization of the molecular conformation and red-shifting their PL spectra. We can explain this mechanism from the XRD and DSC studies. XRD patterns of the two as-synthesized samples clearly show intensive and sharp reflection peaks, hinting at a well-ordered crystalline structure. In contrast, the XRD profiles of the ground samples exhibit a weak, broad, and diffuse peak (Figure S2c and Figure S3c, Supporting Information), indicating that the molecule packing patterns had become an amorphous structure after grinding. As anticipated, the DSC curves of the two ground samples show an exothermic peak around 86 and 123 °C, respectively (Figure S2d and Figure S3d, Supporting Information), indicating the cold−crystallization transition.[75] Nevertheless, no exothermic peak can be detected for the pristine powder before melting (compound **4**, m.p. = 236 °C; compound **5**, m.p. = 315 °C). On the basis of these results, the grinding treatment can transform the thermodynamically stable phase to a metastable state.

Explosive Detection. Sensitive detection of chemical species has become more important for environmental protection and antiterrorist threats.[78−80] Strong PL emission of the luminogens in the aqueous mixtures may be quenched by explosives, which will be indicative of their potential application as chemosensors. With such regard, we examined whether the PL spectra of the as-synthesized samples would change in the presence of explosives. Nitroaromatic compounds such as 2,4-dinitrotoluene, 2,4,6-trinitrotoluene, and 2,4,6-trinitrophenol (picric acid; PA) are warfare explosives. PA was used as a model compound due to its commercial availability. Herein, we study the fluorescence changes of compounds **4** and **6** in response to different amounts of PA in the aqueous mixture (Figure 7a, Figure S4 in the Supporting Information).

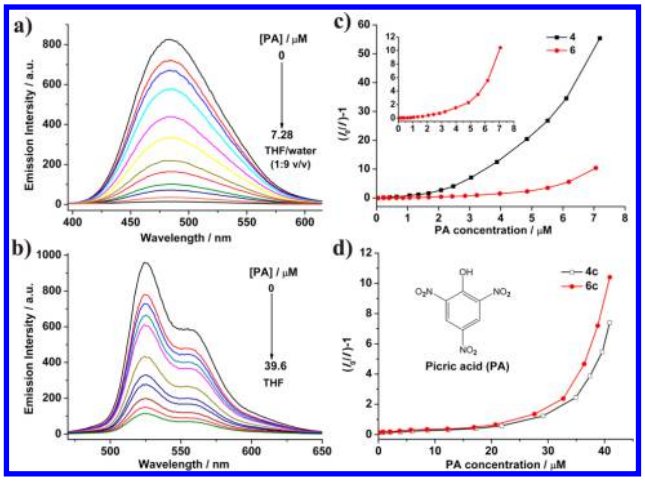

Figure 7. Emission spectra of (a) compound **4** in THF/water mixture (1:9, v/v) and (b) compound **4c** in THF solution with the addition of different amounts of PA. Compound concentration: 10 μM. Stern−Volmer plots of $(I_0/I - 1)$ values versus [PA] of (c) compounds **4** and **6** in THF/water mixture (1:9, v/v) and (d) compounds **4c** and **6c** in pure THF solution. I = peak intensity and I_0 = peak intensity at [PA] = 0 μM. Inset in panel b: enlarged plot of compound 6 in THF/water mixture (1:9, v/v).

As shown in Figure 7a, the emission of compound **4** is progressively weakened when an increasing amount of PA is added into its nanoaggregates in the aqueous mixture. The fluorescence quenching can be clearly discerned at a PA level as low as 0.5 μM or 0.3 ppm. When the PA concentration is increased to 7.28 μM, virtually no luminescence can be detected by the spectrofluorometer. The Stern−Volmer plots of relative PL intensity $(I_0/I - 1)$ versus PA concentration are shown in Figure 7c to further quantify the quenching efficiency, with very high Stern−Volmer quenching constants of about 8.98×10^5 M^{-1} and 3.53×10^5 M^{-1} for compounds **4** and **6** in the THF/water mixture (1:9 by volume), respectively, in the low PA concentration range. The very rapid fluorescence quenching response of the two compounds can be explained by the efficient photoinduced electron transfer and/or energy transfer quenching process.[81,82] Because the electron-deficient PA is a strong quencher of the fluorescence of electron-rich

dx.doi.org/10.1021/cm501590w | Chem. Mater. 2014, 26, 4221−4229

compounds **4** and **6** via an electron transfer process, the close vicinity between the compounds and PA in the nanoaggregates system can greatly promote the electron transfer process. On the other hand, the absorption of PA overlaps with the PL spectra of the luminogens in a wavelength region of 395−485 nm (Figure S6, Supporting Information), which facilitates the energy transfer from the excited states of the luminogens to the ground state of PA, thus further enhancing the fluorescence quenching efficiency.

After oxidizing compound **4** to a less twisted molecule, as above-noted, the product can emit strongly in the neat solvent. So we continued to research whether the slightly twisted compounds **4c** and **6c** in pure THF solvent can be utilized as chemosensors (Figure 7b, Figure S5 in the Supporting Information). The near-planar molecule has a more impacted packing pattern than the twisted molecule before being oxidized, which may facilitate the electron transfer because of the strong π-stacking interactions. As we expected, the PL spectrum of compound **4c** is weakened when the PA is gradually added into its THF solution and is almost completely quenched in the presence of a large amount of PA up to 39.6 μM (Figure 7c). In addition, the two near-planar molecules exhibit almost identical responses to quenching by PA (Figure 7d), with respective quenching constants as large as 1.96×10^4 M^{-1} and 3.11×10^4 M^{-1} for compound **4c** and compound **6c**. Similar to the compounds **4** and **6**, the Stern−Volmer plots of **4c** and **6c** in THF solution bend upward instead of being straight lines, indicating a superamplification quenching effect. A possible reason may be that the PL emission is quenched by static quenching or static and dynamic quenching participates in it simultaneously.[83] Measuring the lifetimes of the luminogen in the absence or presence of the quencher can be used as one method to determine whether the quenching mechanism is dynamic, static, or both of them. The fluorescence lifetime is truncated by dynamic quenching due to the collision of quencher molecules with excited molecules of the luminogen but unaffected by static quenching because of the formation of a nonemissive luminogen−quencher complex.[84,85] As shown in Figure S7 in the Supporting Information, the fluorescence lifetime changes little along with increasing PA concentration in the solution, suggesting that the excitons mainly decay via the static pathway. Evidently, the extremely high sensitivity of these TPE derivatives for PA detection made them promising candidates as chemosensors.

Cell Imaging Application. To evaluate the performance of the samples in living cells, we choose luminogens **4** and **4b** as representatives owing to the different emission color and good dispersion in dimethyl sulfoxide (DMSO) buffer solution. Confocal laser scanning microscopy was used to record the mouse fibroblast cells (L929) cultured with the luminogens for 4 h. The confocal images illustrated that almost all of the cells can be uniformly labeled by using these luminogens (Figure 8). The images of L929 cells reveal that the chromophores selectively stain the cytoplasm of the living cells but not their nucleus regions, probably due to their hydrophobic nature.

As biomaterials, cytotoxicity of these dyes must be controlled due to their potential side effect during imaging in cells or tissues. So the 3-(4,5-dimethylthiazol-2-yl)-2,5-diphenyltetrazolium bromide (MTT) assay was performed to ascertain the cytotoxic effect of these dyes. This is a general method to reflect the mitochondrial activity of cells and represents a parameter for their metabolic activity. Figure 9 shows the cell viability for L929 cells treated with the as-synthesized dyes at different

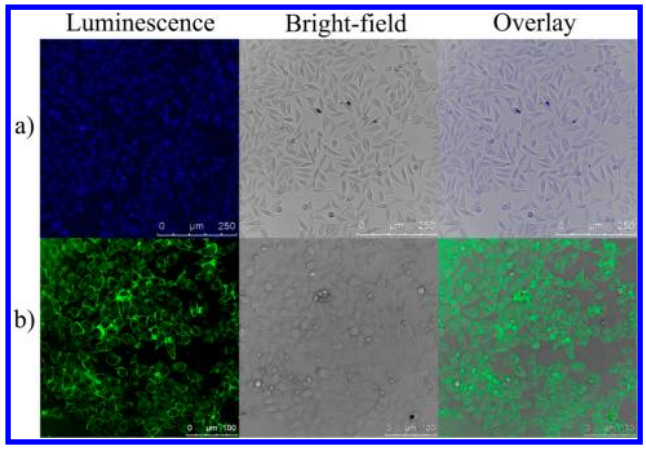

Figure 8. Confocal imaging of L929 cells incubated with **4** (a) and **4b** (b) with a concentration of 20 μM for 4 h at 37 °C.

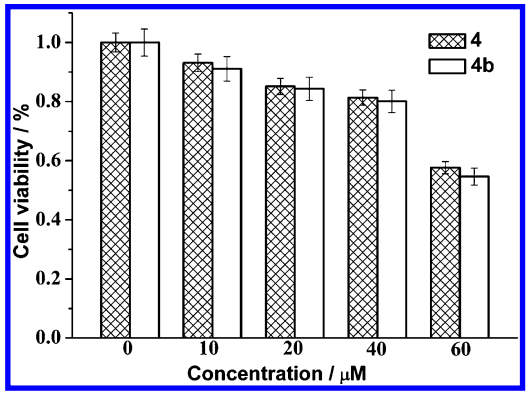

Figure 9. Cell viability of L929 cells incubated with different concentrations of **4** and **4b** for 24 h, respectively.

concentrations for 24 h. Average cell viability was above 90% after 24 h of culturing with the dyes at the concentration of 10 μM. The results clearly indicate that the prepared dyes have little toxic effects on living cells at low micromolar concentrations. Here, further incorporation of the blue and green luminogens into living cells can be explored for multicolor bioimaging due to their strong fluorescence and low toxicity.

■ CONCLUSIONS

In summary, we have synthesized and fully characterized a series of graphene-like molecules based on TPEs. The ring planarity dramatically alters the luminescence behaviors of the twisted conjugated precursors. UV and PL spectra were obtained to quantify this change. After the ring-closing reaction, the emission maximum is red-shifted evidently compared to the starting sample. That is to say, the extent of the blockage of intramolecular rotation of the phenyl blades can determine its emission property. CV results demonstrate the order of the conjugation length. Interestingly, compound **6c** can self-assemble into one-dimensional microfibers with the hexagon-like shape. Compounds **1**, **4**, and **5** exhibit obvious piezofluorochromic behaviors generated through changing the structure of molecular assemblies under external pressure. The samples before and after oxidation can serve as an efficient sensor for the detection of picric acid under different conditions, with the quenching constant and the detection limit being up to 8.98×10^5 M^{-1} and 0.3 ppm, respectively,

dx.doi.org/10.1021/cm501590w | *Chem. Mater.* 2014, 26, 4221−4229

suggesting that they are promising candidates for a wide range of high-tech applications. Furthermore, we also demonstrated that the as-synthesized molecules can be utilized as a fluorescence marker in bioimaging due to their excellent biocompatibility and low toxicity.

■ ASSOCIATED CONTENT

Supporting Information

Synthetic procedures and characterization data of all new compounds, crystal structure data for **1** and **6** (CCDC 966661 and 966662) (CIF file), optical properties of compounds **4**−**6c**, cyclic voltammograms of compounds **6** and **6c**, photographs under UV illumination, PL spectra, DSC thermograms, powder XRD patterns of **4** and **5** in different aggregation states, the changes of PL spectra of compounds **6** and **6c** with different amounts of PA, fluorescence decay of **4**, **6**, **4c**, and **6c** aggregates against the concentration of PA, ^{1}H NMR AND ^{13}C NMR spectra, and MALDI-TOF of compounds **4**−**6c**. This material is available free of charge via the Internet at http://pubs.acs.org/.

■ AUTHOR INFORMATION

Corresponding Author

*E-mail: weizhiwang@fudan.edu.cn. Tel.: +86 21-65643836.

Notes

The authors declare no competing financial interest.

■ ACKNOWLEDGMENTS

This work was financially supported by the National Natural Science Foundation of China (21274027 and 20974022).

■ REFERENCES

(1) Slonczewski, J. C.; Weiss, P. R. *Phys. Rev.* **1958**, *109*, 272−279.
(2) Geim, A. K.; Novoselov, K. S. *Nat. Mater.* **2007**, *6*, 183−191.
(3) Zhang, Y.; Tan, Y.; Stormer, H. L.; Kim, P. *Nature* **2005**, *438*, 201−204.
(4) Heersche, H. B.; Jarillo-Herrero, P.; Oostinga, J. B.; Vandersypen, L. M. K.; Morpurgo, A. F. *Nature* **2007**, *446*, 56−59.
(5) Balandin, A. A.; Ghosh, S.; Bao, W.; Calizo, I.; Teweldebrhan, D.; Miao, F.; Lau, C. N. *Nano Lett.* **2008**, *8*, 902−907.
(6) Mak, K. F.; Sfeir, M. Y.; Wu, Y.; Lui, C. H.; Misewich, J. A.; Heinz, T. F. *Phys. Rev. Lett.* **2008**, *101*, 196405.
(7) Bonaccorso, F.; Sun, Z.; Hasan, T.; Ferrari, A. C. *Nat. Photonics* **2010**, *4*, 611−622.
(8) He, T.; Wei, W.; Ma, L.; Chen, R.; Wu, S.; Zhang, H.; Yang, Y.; Ma, J.; Huang, L.; Gurzadyan, G. G. *Small* **2012**, *8*, 2163−2168.
(9) Lim, G.; Chen, Z.; Clark, J.; Goh, R. G.; Ng, W.; Tan, H.; Friend, R. H.; Ho, P. K.; Chua, L. *Nat. Photonics* **2011**, *5*, 554−560.
(10) Lee, C.; Wei, X.; Kysar, J. W.; Hone, J. *Science* **2008**, *321*, 385−388.
(11) Ruoff, R. *Nat. Nanotechnol.* **2008**, *3*, 10−11.
(12) Park, S.; Ruoff, R. S. *Nat. Nanotechnol.* **2009**, *4*, 217−224.
(13) Singh, V.; Joung, D.; Zhai, L.; Das, S.; Khondaker, S. I.; Seal, S. *Prog. Mater. Sci.* **2011**, *56*, 1178−1271.
(14) Soldano, C.; Mahmood, A.; Dujardin, E. *Carbon* **2010**, *48*, 2127−2150.
(15) Kuila, T.; Bose, S.; Mishra, A. K.; Khanra, P.; Kim, N. H.; Lee, J. H. *Prog. Mater. Sci.* **2012**, *57*, 1061−1105.
(16) Novoselov, K. S.; Geim, A. K.; Morozov, S. V.; Jiang, D.; Zhang, Y.; Dubonos, S. V.; Grigorieva, I. V.; Firsov, A. A. *Science* **2004**, *306*, 666−669.
(17) Hernandez, Y.; Nicolosi, V.; Lotya, M.; Blighe, F. M.; Sun, Z.; De, S.; McGovernI, T.; Holland, B.; Byrne, M.; Gun'Ko, Y. K.; Boland, J. J.; Niraj, P.; Duesberg, G.; Krishnamurthy, S.; Goodhue, R.; Hutchison, J.; Scardaci, V.; Ferrari, A. C.; Coleman, J. N. *Nat. Nanotechnol.* **2008**, *3*, 563−568.
(18) Su, C.; Lu, A.; Xu, Y.; Chen, F.; Khlobystov, A. N.; Li, L. *ACS Nano* **2011**, *5*, 2332−2339.
(19) Reina, A.; Jia, X.; Ho, J.; Nezich, D.; Son, H.; Bulovic, V.; Dresselhaus, M. S.; Kong, J. *Nano Lett.* **2008**, *9*, 30−35.
(20) Wu, B.; Geng, D.; Guo, Y.; Huang, L.; Xue, Y.; Zheng, J.; Chen, J.; Yu, G.; Liu, Y.; Jiang, L.; Hu, W. *Adv. Mater.* **2011**, *23*, 3522−3525.
(21) Berger, C.; Song, Z.; Li, X.; Wu, X.; Brown, N.; Naud, C.; Mayou, D.; Li, T.; Hass, J.; Marchenkov, A. N.; Conrad, E. H.; First, P. N.; de Heer, W. A. *Science* **2006**, *312*, 1191−1196.
(22) Huang, H.; Chen, W.; Chen, S.; Wee, A. T. S. *ACS Nano* **2008**, *2*, 2513−2518.
(23) Zhang, W.; Cui, J.; Tao, C. A.; Wu, Y.; Li, Z.; Ma, L.; Wen, Y.; Li, G. *Angew. Chem., Int. Ed.* **2009**, *48*, 5864−5868.
(24) Wu, J.; Pisula, W.; Müllen, K. *Chem. Rev.* **2007**, *107*, 718−747.
(25) Zhi, L.; Müllen, K. *J. Mater. Chem.* **2008**, *18*, 1472−1484.
(26) Clar, E.; Stewart, D. G. *J. Am. Chem. Soc.* **1953**, *75*, 2667−2672.
(27) Clar, E.; Schmidt, W. *Tetrahedron* **1979**, *35*, 2673−2680.
(28) Scholl, R.; Seer, C. *Chem. Ber.* **1922**, *55*, 330−341.
(29) Zander, M. *Polycyclische Aromaten*; B. G. Teubner: Stuttgart, 1995.
(30) Feng, X.; Wu, J.; Enkelmann, V.; Müllen, K. *Org. Lett.* **2006**, *8*, 1145−1148.
(31) Simpson, C. D.; Mattersteig, G.; Martin, K.; Gherghel, L.; Bauer, R. E.; Räder, H. J.; Müllen, K. *J. Am. Chem. Soc.* **2004**, *126*, 3139−3147.
(32) Navale, T. S.; Thakur, K.; Rathore, R. *Org. Lett.* **2011**, *13*, 1634−1637.
(33) Wolf, M. O.; Fox, H. H.; Fox, M. A. *J. Org. Chem.* **1996**, *61*, 287−294.
(34) Schreivogel, A.; Maurer, J.; Winter, R.; Baro, A.; Laschat, S. *Eur. J. Org. Chem.* **2006**, *2006*, 3395−3404.
(35) Sun, Y. P.; Fox, M. A. *J. Am. Chem. Soc.* **1993**, *115*, 747−750.
(36) Schuddeboom, W.; Jonker, S. A.; Warman, J. M.; de Haas, M. P.; Vermeulen, M. J.; Jager, W. F.; de Lange, B.; Feringa, B. L.; Fessenden, R. W. *J. Am. Chem. Soc.* **1993**, *115*, 3286−3290.
(37) Ma, J.; Dutt, G. B.; Waldeck, D. H.; Zimmt, M. B. *J. Am. Chem. Soc.* **1994**, *116*, 10619−10629.
(38) Ito, A.; Nakano, Y.; Kato, T.; Tanaka, K. *Chem. Commun.* **2005**, 403−405.
(39) Mori, T.; Inoue, Y. *J. Phys. Chem. A* **2005**, *109*, 2728.
(40) Liu, L.; Zhang, G.; Xiang, J.; Zhang, D.; Zhu, D. *Org. Lett.* **2008**, *10*, 4581−4584.
(41) Luo, J.; Xie, Z.; Lam, J. W. Y.; Cheng, L.; Chen, H.; Qiu, C.; Kwok, H. S.; Zhan, X.; Liu, Y.; Zhu, D.; Tang, B. Z. *Chem. Commun.* **2001**, 1740−1741.
(42) Zhao, Z.; Lam, J. W. Y.; Tang, B. Z. *J. Mater. Chem.* **2012**, *22*, 23726−23740.
(43) Zhao, Z.; Lam, J. W. Y.; Tang, B. Z. *Curr. Org. Chem.* **2010**, *14*, 2109−2132.
(44) Zhao, Z.; Chen, S.; Shen, X.; Mahtab, F.; Yu, Y.; Lu, P.; Lam, J. W. Y.; Kwok, H. S.; Tang, B. Z. *Chem. Commun.* **2010**, *46*, 686−688.
(45) Vyas, V. S.; Rathore, R. *Chem. Commun.* **2010**, *46*, 1065−1067.
(46) Wang, J.; Mei, J.; Hu, R.; Sun, J. Z.; Qin, A.; Tang, B. Z. *J. Am. Chem. Soc.* **2012**, *134*, 9956−9966.
(47) Wang, W.; Lin, T.; Wang, M.; Liu, T.; Ren, L.; Chen, D.; Huang, S. *J. Phys. Chem. B* **2010**, *114*, 5983−5988.
(48) Hong, Y.; Lam, J. W. Y.; Tang, B. Z. *Chem. Soc. Rev.* **2011**, *40*, 5361−5388.
(49) Zhao, Z.; Chen, S.; Lam, J. W. Y.; Jim, C. K. W.; Chan, C. Y. K.; Wang, Z.; Lu, P.; Deng, C.; Kwok, H. S.; Ma, Y.; Tang, B. Z. *J. Phys. Chem. C* **2010**, *114*, 7963−7972.
(50) Zhou, J.; Chang, Z.; Jiang, Y.; He, B.; Du, M.; Lu, P.; Hong, Y.; Kwok, H. S.; Qin, A.; Qiu, H.; Zhao, Z.; Tang, B. Z. *Chem. Commun.* **2013**, *49*, 2491−2493.
(51) Jayanty, S.; Radhakrishnan, T. P. *Chem.—Eur. J.* **2004**, *10*, 791−797.

(52) Wang, Z.; Shao, H.; Ye, J.; Tang, L.; Lu, P. *J. Phys. Chem. B* **2005**, *109*, 19627−19633.
(53) Itami, K.; Ohashi, Y.; Yoshida, J. *J. Org. Chem.* **2005**, *70*, 2778−2792.
(54) Bhongale, C. J.; Hsu, C. S. *Angew. Chem., Int. Ed.* **2006**, *45*, 1404−1408.
(55) Shi, J.; Chang, N.; Li, C.; Mei, J.; Deng, C.; Luo, X.; Liu, Z.; Bo, Z.; Dong, Y. Q.; Tang, B. Z. *Chem. Commun.* **2012**, *48*, 10675−10677.
(56) Müller, M.; Kübel, C.; Müllen, K. *Chem.—Eur. J.* **1998**, *4*, 2099−2109.
(57) Dötz, F.; Brand, J. D.; Ito, S.; Gherghel, L.; Müllen, K. *J. Am. Chem. Soc.* **2000**, *122*, 7707−7717.
(58) Cai, J.; Ruffieux, P.; Jaafar, R.; Bieri, M.; Braun, T.; Blankenburg, S.; Muoth, M.; Seitsonen, A. P.; Saleh, M.; Feng, X.; Müllen, K.; Fasel, R. *Nature* **2010**, *466*, 470−473.
(59) Hoeben, F. J.; Jonkheijm, P.; Meijer, E. W.; Schenning, A. P. *Chem. Rev.* **2005**, *105*, 1491−1546.
(60) Zhao, Z.; Li, J.; Chen, X.; Lu, P.; Yang, Y. *Org. Lett.* **2008**, *10*, 3041−3044.
(61) Li, X. Q.; Zhang, X.; Ghosh, S.; Würthner, F. *Chem.—Eur. J.* **2008**, *14*, 8074−8078.
(62) Zang, L.; Che, Y.; Moore, J. S. *Acc. Chem. Res.* **2008**, *41*, 1596−1608.
(63) Toal, S. J.; Jones, K. A.; Magde, D.; Trogler, W. C. *J. Am. Chem. Soc.* **2005**, *127*, 11661−11665.
(64) Ning, Z.; Chen, Z.; Zhang, Q.; Yan, Y.; Qian, S.; Cao, Y.; Tian, H. *Adv. Funct. Mater.* **2007**, *17*, 3799−3807.
(65) Pucci, A.; Di Cuia, F.; Signori, F.; Ruggeri, G. *J. Mater. Chem.* **2007**, *17*, 783−790.
(66) Olson, C. E.; Previte, M. J. R.; Fourkas, J. T. *Nat. Mater.* **2002**, *1*, 225−228.
(67) Kishimura, A.; Yamashita, T.; Yamaguchi, K.; Aida, T. *Nat. Mater.* **2005**, *4*, 546−549.
(68) Sagara, Y.; Mutai, T.; Yoshikawa, I.; Araki, K. *J. Am. Chem. Soc.* **2007**, *129*, 1520−1521.
(69) Sagara, Y.; Kato, T. *Nat. Chem.* **2009**, *1*, 605−610.
(70) Zhao, Y.; Gao, H.; Fan, Y.; Zhou, T.; Su, Z.; Liu, Y.; Wang, Y. *Adv. Mater.* **2009**, *21*, 3165−3169.
(71) Zhang, G.; Lu, J.; Sabat, M.; Fraser, C. L. *J. Am. Chem. Soc.* **2010**, *132*, 2160−2162.
(72) Luo, X.; Li, J.; Li, C.; Heng, L.; Dong, Y. Q.; Liu, Z.; Bo, Z.; Tang, B. Z. *Adv. Mater.* **2011**, *23*, 3261−3265.
(73) Yoon, S.; Park, S. *J. Mater. Chem.* **2011**, *21*, 8338−8346.
(74) Li, H.; Zhang, X.; Chi, Z.; Xu, B.; Zhou, W.; Liu, S.; Zhang, Y.; Xu, J. *Org. Lett.* **2011**, *13*, 556−559.
(75) Xu, B.; Chi, Z.; Zhang, X.; Li, H.; Chen, C.; Liu, S.; Zhang, Y.; Xu, J. *Chem. Commun.* **2011**, *47*, 11080−11082.
(76) Chi, Z.; Zhang, X.; Xu, B.; Zhou, X.; Ma, C.; Zhang, Y.; Liu, S.; Xu, J. *Chem. Soc. Rev.* **2012**, *41*, 3878−3896.
(77) Luo, X.; Zhao, W.; Shi, J.; Li, C.; Liu, Z.; Bo, Z.; Dong, Y. Q.; Tang, B. Z. *J. Phys. Chem. C* **2012**, *116*, 21967−21972.
(78) Steinfeld, J. I.; Wormhoudt, J. *Annu. Rev. Phys. Chem.* **1998**, *49*, 203−232.
(79) Sohn, H.; Sailor, M. J.; Magde, D.; Trogler, W. C. *J. Am. Chem. Soc.* **2003**, *125*, 3821−3830.
(80) Sanchez, J. C.; DiPasquale, A. G.; Rheingold, A. L.; Trogler, W. C. *Chem. Mater.* **2007**, *19*, 6459−6470.
(81) Li, D.; Liu, J.; Kwok, R. T. K.; Liang, Z.; Tang, B. Z.; Yu, J. *Chem. Commun.* **2012**, *48*, 7167−7169.
(82) Fang, Q.; Geng, J.; Liu, B.; Gao, D.; Li, F.; Wang, Z.; Guan, G.; Zhang, Z.; Zhang, Z. *Chem.—Eur. J.* **2009**, *15*, 11507−11514.
(83) Liu, J.; Zhong, Y.; Lu, P.; Hong, Y.; Lam, J. W. Y.; Faisal, M.; Yu, Y.; Wong, K. S.; Tang, B. Z. *Polym. Chem.* **2010**, *1*, 426−429.
(84) Lu, P.; Lam, J. W. Y.; Liu, J.; Jim, C. K.; Yuan, W.; Xie, N.; Zhong, Y.; Hu, Q.; Wong, K. S.; Cheuk, K. K. *Macromol. Rapid Commun.* **2010**, *31*, 834−839.
(85) An, Z. F.; Zheng, C.; Chen, R. F.; Yin, J.; Xiao, J. J.; Shi, H. F.; Tao, Y.; Qian, Y.; Huang, W. *Chem.—Eur. J.* **2012**, *18*, 15655−15661.